Light Source Notes

Assigned Number: LSBL-621

Date of Entry: 5/23/2002

Publishing Date: 5/2002

Author(s): T. Ernest Glover, Philip A. Heimann, Robert W. Schoenlein

Title: Beamline 5.3.1 Torroidal-Mirror Scattering Profile

Other Number(s):

Beamline 5.3.1 Torroidal-Mirror Scattering Profile

T. Ernest Glover, Philip A. Heimann, Robert W. Schoenlein

May 2002

Introduction

Successful utilization of "sliced" femtosecond x-rays on beamline 5.3.1 requires that one minimizes scattering in the horizontal plane due to the M1 focusing torrid. Scattering constitutes a background upon which the sliced xrays sit and femtosecond experiments become unfeasible if the background (picosecond) xray flux is large compared to the femtosecond xray flux. This becomes evident by noting that if a signal sits on top of a background which is N times larger than the desired signal, then the data acquisition time required to achieve a given signal-to-noise ratio increases by a factor of 1+N (appendix A). Since slicing extracts ~$4x10^{-4}$ of the picosecond x-ray bunch (~100 fs slice out of ~ 50 ps bunch with ~20% slicing efficiency) we would like the level of horizontal scattering (at 400-500 um from beam center) to be $4x10^{-4}$ or less; here a perfect (scatter free) mirror would only decrease the data acquisition time by a factor of two.

Beam profile measurements were performed on the *original* 5.3.1 torroid to assess the level of scattering in the horizontal plane. The M1 torroid was adjusted to produce an image close to the 1:1 imaging point, adjustable horizontal and vertical slits were placed at this image point and a Si photodiode (AXUV-100) and current amplifier were used to detect the transmitted x-rays as a function of slit position. The vertical slits were centered on the vertical beam position and offered a 300 um aperture while the horizontal slits (at 50 um aperture) were scanned. Care was taken to ensure that neither the photodiode not the current amplifier saturated during the measurements. Additionally, as detailed below, filters may have been inserted into the beam. A 250 um Be filter (~1 m upstream) and/or a 1 mm Al filter (directly in front of the photodiode) may have been used.

Beam Profile Data

White Beam

White beam measurements were performed with several attenuators in the beam in order to achieve a linear response from the photodiode. The attenuators included : 1 mm Al filter in front of the photodiode, air in the experimental chamber (~50 cm air path, 1 atm pressure), a 250 um Be window in the beam. Additionally, the white beam spectrum is modified by the reflectivity of the Pt-coated M1 mirror (5 mrad grazing angle). The spectral response of these elements is shown in Figure 1.a. The bend magnet spectrum before and after these spectral corrections is shown in Figure 1.b. The spectrum after corrections is shown to peak at 15 keV and has a spectral width (FWHM) of 5 keV.

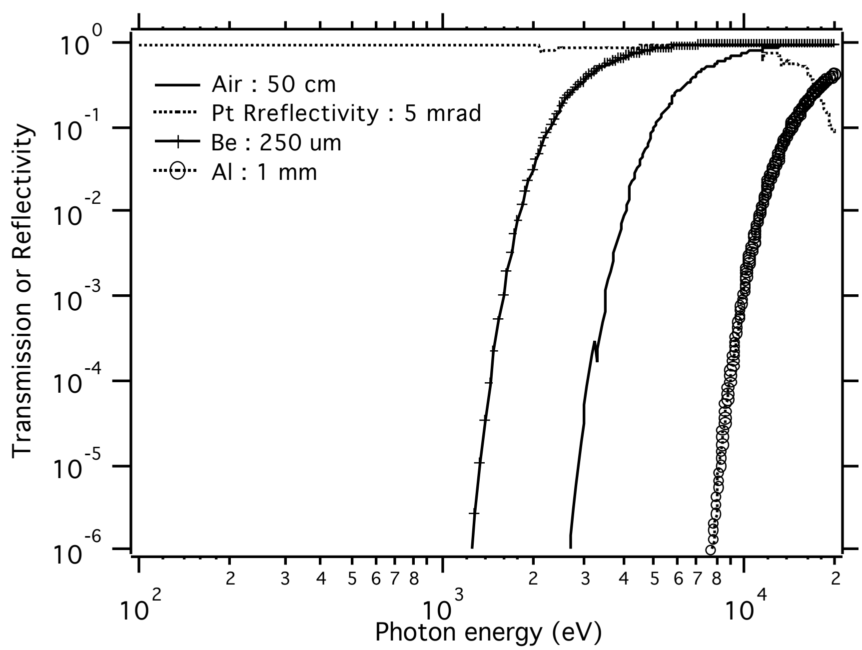

Figure 1.a Spectral corrections

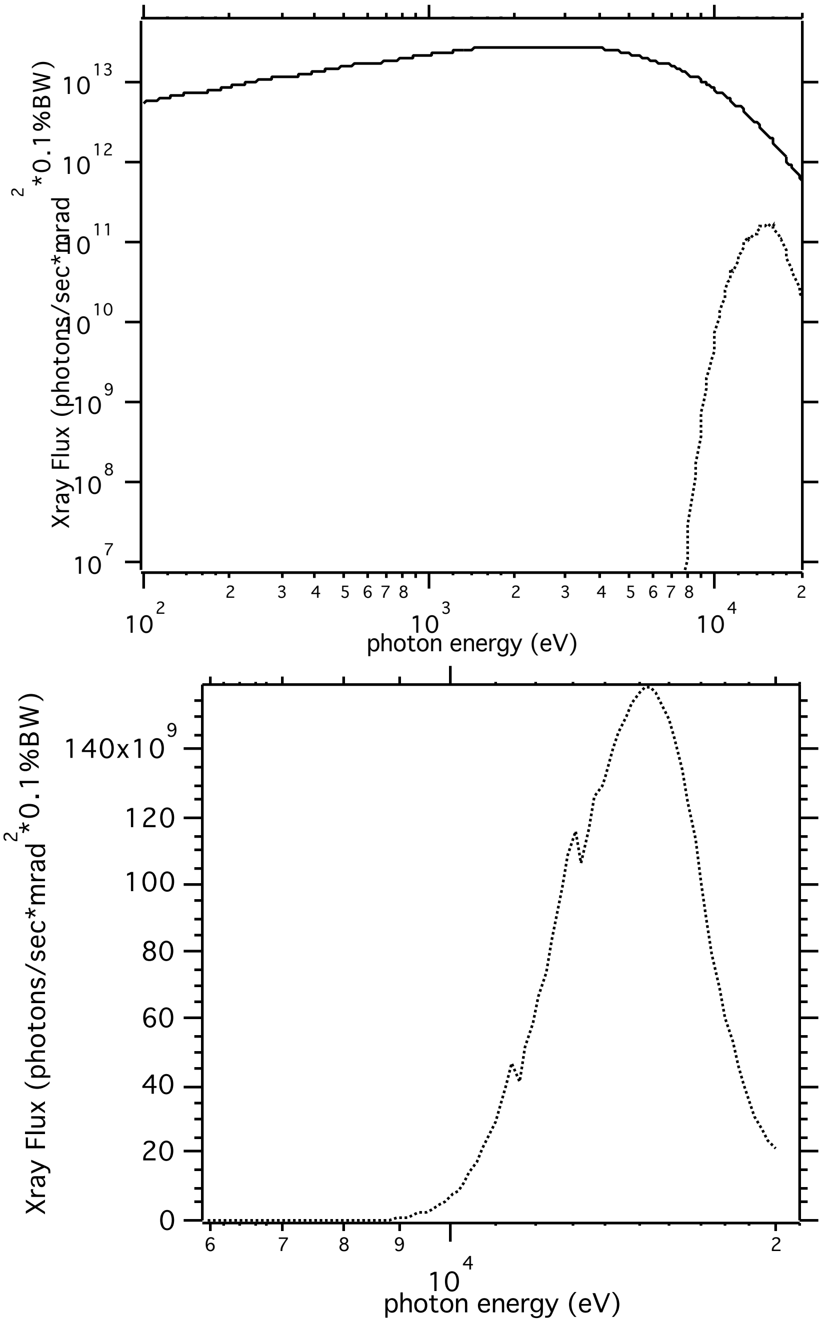

Figure 1.b Bend magnet flux before (solid line) and after (dashed line) spectral corrections.

Figure 2 shows the measured white-beam profile. The curves have been background subtracted (x-ray shutter closed to establish background level). The solid curve emphasizes the overall beam profile (beam peak, center etc.) and has been multiplied by a factor of 1000 (current amplifier was 20 uA/V in this case). A gaussian fit to this curve (dashed curve) shows that the horizontal spot is 243 um FWHM and is centered at 0 um.

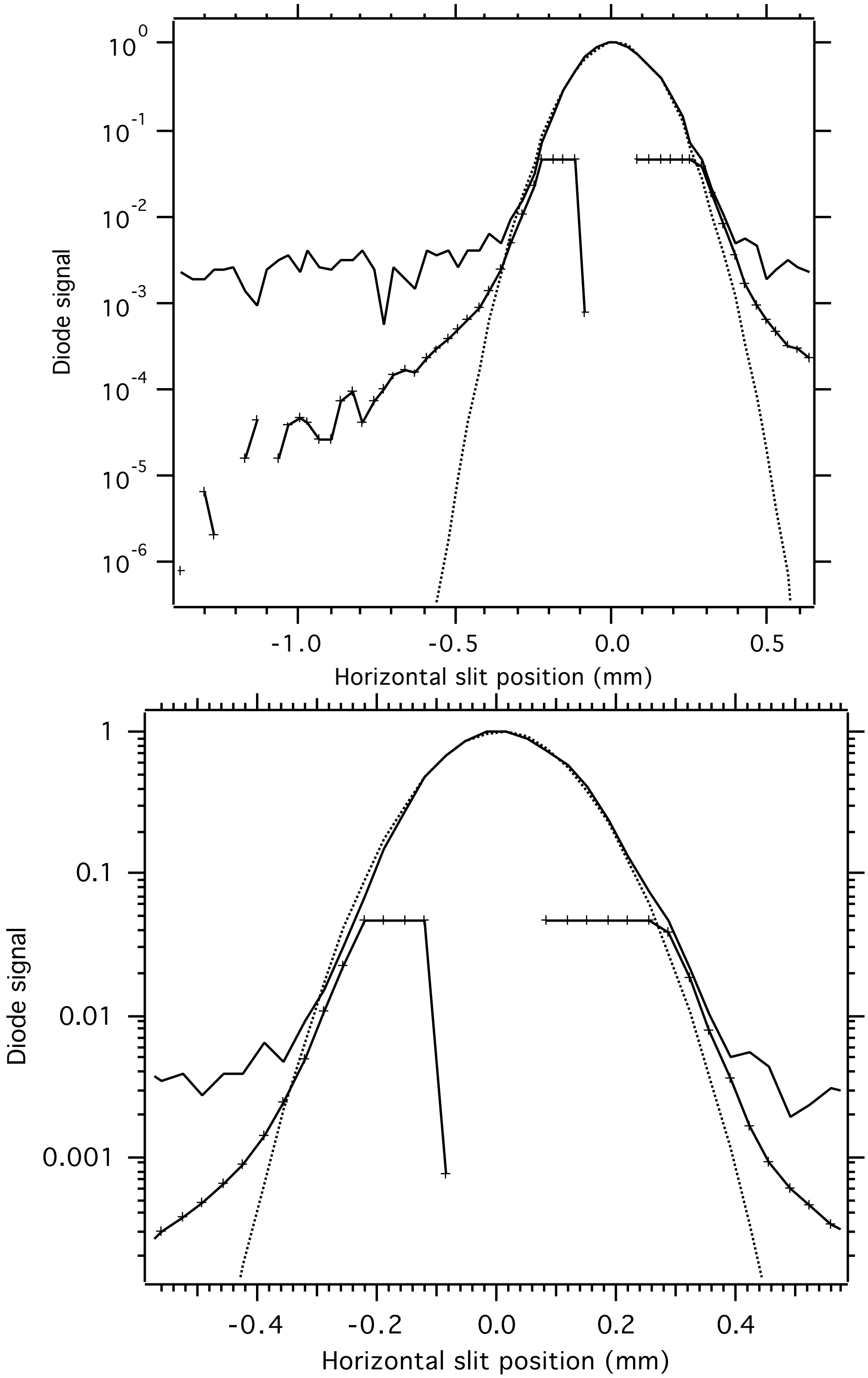

Figure 2. Horizontal beam profile (white beam).

The solid curve with markers emphasizes the spatial wings and is obtained with the current amplifier set to 20 nA/V. We note that the signal 'drop-outs' in this curve are due either to intentionally closing the xray shutter (to determine the zero level) or to the combination of background subtraction along with signal fluctuations.

Figure 2 indicates that the beam profile becomes non-gaussian ~365 um from beam center. We next specify the level of scatter 400 um and 500 um from beam center. The peak signal (i.e. signal at 0 um) is 148.34 units. The signal 500 um from beam center is 0.207 units and indicates a ratio:

$$Wing_{500} / Peak = 4.9x10^{-4}$$

The scattered light level increases as we move closer to beam center. The signal 400 um from beam center is 0.072 units and indicates a ratio :

$$Wing_{400} / Peak = 1.4x10^{-3}$$

A second set of measurements, taken several days later but under nominally the same conditions, indicates a horizontal beam size is 310 um (FWHM). The peak signal is 74.34 units. The signal 500 um from beam center is 0.018 units and indicates a ratio:

$$Wing_{500} / Peak = 2.4x10^{-4}$$

The signal 400 um from beam center is 0.107 units and indicates a ratio :

$$Wing_{400} / Peak = 1.4x10^{-3}$$

The two measurements are therefore consistent to within a factor of two and we note that removing the Be window did not appreciably change the level of scattering.

Quasi-Monochromatic Beam

Finally we consider measurements performed using quasi-monochromatic beam. Here multilayer mirrors are inserted into the 5.3.1 monochrometer and we measure the beam profile at a wavelength of 5 keV. The multilayer mirrors are manufactured at the Center for Xray Optics, LBNL (substrate ~300 um thick). The W/B_4C multilayers have a 4 nm period and the forty-period multilayer bandwidth was measured to be ~1% (FWHM). We note that the peak-to-wing ratios mentioned below did not change with a ~500 eV change in center wavelength. While the 250 um Be filter was used for these measurements, the 1 mm Al filter was not used and the system was evacuated.

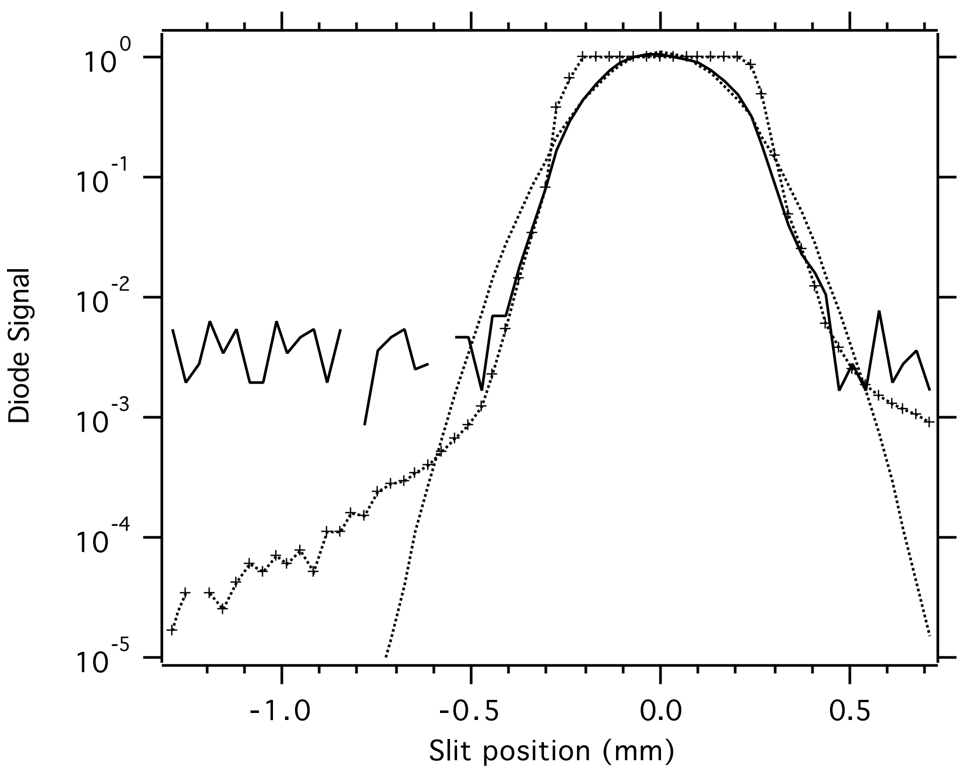

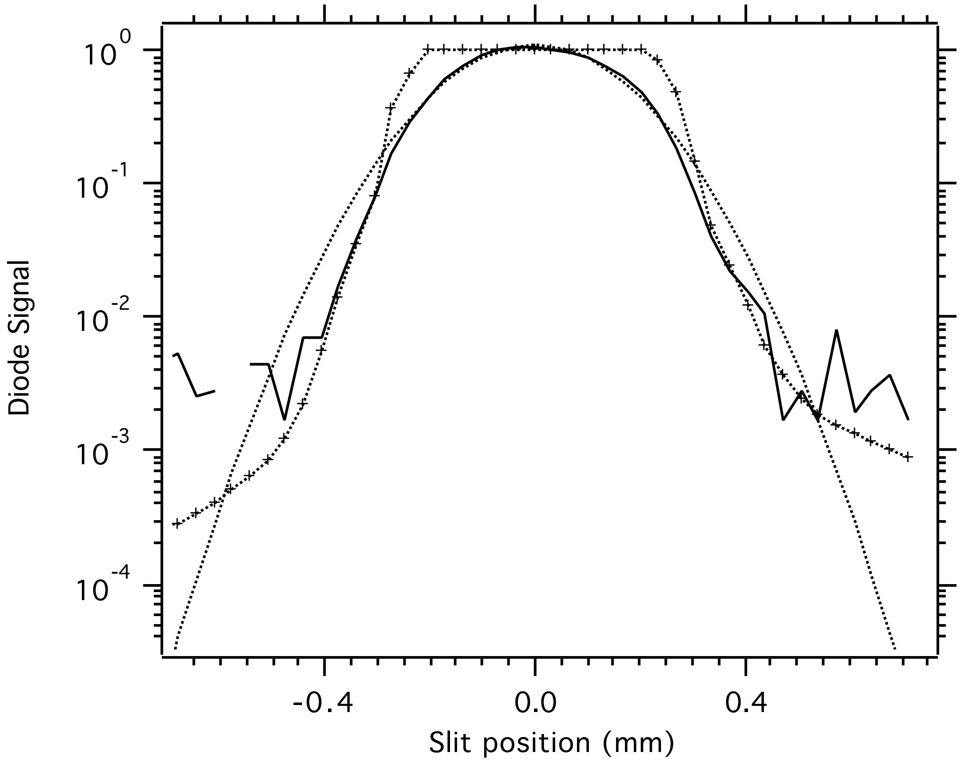

Figure 3. Horizontal beam profile (5 keV).

The beam profile curves have been background subtracted and a factor of 100 scaling has been applied to the solid curve. A gaussian fit (dashed curve) indicates that the horizontal spot is 353 um FWHM and the peak signal is 7.4 units. The large beam size indicates that it is likely that the multilayer substrate is warped; either in the manufacturing process or from experimental factors such as mounting stress and/or thermal loading.

Figure 3 indicates that the beam profile becomes non-gaussian ~275 um from beam center. The signal 500 um from beam center is 0.0066 units and indicates a ratio:

$$\text{Wing}_{500} \,/\, \text{Peak} = 9\text{x}10^{-4}$$

The signal 400 um from beam center is 0.053 units and indicates a ratio :

$$\text{Wing}_{400} \,/\, \text{Peak} = 7\text{x}10^{-3}$$

These measurements indicate that the scattering is significantly worse as compared to the white beam measurements.

Summary

Scattering in the horizontal plane was assessed by measuring the horizontal beam profile over a dynamic range of $\sim 10^4$. Measurements were made using white beam (effective spectrum peaked @ ~15 keV) and using quasi-monochromatic beam (5 keV). White beam showed the best peak-to-wing ratio : $\sim 3.6 \times 10^{-4}$ ($\pm 1.3 \times 10^{-4}$) at 500 um from beam center and 1.4×10^{-3} at 400 um from beam center. The scattering levels obtained with multilayer mirrors are : 9×10^{-4} at 500 um from beam center and 7×10^{-3} at 400 um from beam center.

The measured scattered-light levels indicated that it is reasonably efficient to use femtosecond xrays in a 'white beam' configuration; white beam is directed onto a sample and the transmitted/reflected beam is then spectrally resolved. In this experimental configuration if the sliced x-rays are 500 um off beam center then the ratio of the picosecond-background flux to the femtosecond-x-ray flux is N~1; here femtosecond data can be efficiently recorded with data acquisition times increased by only a factor of two as compared to the ideal-mirror case. If instead sliced x-rays are 400 um off beam center then the ratio of picosecond-to-femtosecond xray flux is N~3.5 and the data acquisition efficiency is compromised (acquisition times increase by a factor of 4.5 compared to the ideal mirror case).

Utilization of femtosecond xrays with monochromatic beam is feasible if the sliced pulses are 500 um off beam center (N~2.25, factor of 3.25 increase in acquisition time) and not feasible if they are only 400 um off beam center (N~17.5, factor of 18.5 increase in acquisition time). Additional work is necessary to determine how lower scattering levels can be obtained with the monochrometer. The additional scattering could be due, for instance, to surface roughness of the multilayers or to scatter generated as the white beam (halo) hits the crystals mounts in the monochrometer.

Appendix A : Increased Data Acquisition Time Due To Background Signal

We consider the increase in data acquisition time if a 'desired' signal sits on top of some background signal. We define the following :

$$A = \text{count rate of the desired signal} \quad (1)$$

$$N{*}A = \text{count rate of the background signal} \quad (2)$$

The total count rate is A + NA = A(1+N) so that the noise level (fluctuations in total counts assuming shot-noise limited detection) is $\sqrt{[A(1+N)]}$. We can now write that the signal-to-noise ratio (S/N) is :

$$S/N = A/\sqrt{[A(1+N)]} = \sqrt{A}/\sqrt{(1+N)} \quad (3)$$

Equation (3) indicates that the presence of background degrades the S/N ratio by a factor of $\sqrt{(1+N)}$. In the absence of background (N=0) we would have a S/N ratio of $\sqrt{A}$. If we regard $\sqrt{A}$ as the desired S/N ratio we see that we must increase the S/N ratio of (3) by a factor of $\sqrt{(1+N)}$ to achieve the ideal ratio. To increase the S/N ratio by a factor of $\sqrt{(1+N)}$ we must increase the data acquisition time by (1+N). We can therefore conclude that if a signal sits on top of a background which is N times larger than the desired signal, then the data acquisition time required to achieve a given signal-to-noise ratio increases by a factor of 1+N.

Appendix B : Data Tables

White Beam Data

Peak	Slit	Wings	Slit
0.00215721	-1.371	8.08952e-07	-1.371
0.00188756	-1.3371	-1.21343e-06	-1.3371
0.00188756	-1.3032	6.60644e-06	-1.3032
0.00229203	-1.26931	2.02238e-06	-1.26931
0.00229203	-1.23541	-5.87839e-05	-1.23541
0.00256168	-1.20151	-2.81785e-05	-1.20151
0.00134825	-1.16761	1.59094e-05	-1.16761
0.000943778	-1.13371	4.35486e-05	-1.13371
0.00229203	-1.09981	-1.63139e-05	-1.09981
0.00310098	-1.06592	1.57746e-05	-1.06592
0.00350546	-1.03202	3.66725e-05	-1.03202
0.00215721	-0.998119	4.67844e-05	-0.998119
0.00390994	-0.96422	4.1661e-05	-0.96422
0.00269651	-0.930322	2.68303e-05	-0.930322
0.00229203	-0.896424	2.61561e-05	-0.896424
0.00310098	-0.862525	7.25361e-05	-0.862525
0.00310098	-0.828627	9.26251e-05	-0.828627
0.00390994	-0.794729	4.03128e-05	-0.794729
0.00229203	-0.76083	7.13226e-05	-0.76083
0.000539302	-0.726932	0.000103007	-0.726932
0.00256168	-0.693034	0.00013914	-0.693034
0.00188756	-0.659136	0.000165296	-0.659136
0.00148308	-0.625237	0.000147903	-0.625237
0.00390994	-0.591339	0.000228529	-0.591339
0.00350546	-0.557441	0.000292841	-0.557441
0.00390994	-0.523542	0.000373601	-0.523542
0.00269651	-0.489644	0.000482675	-0.489644
0.00390994	-0.455746	0.000636511	-0.455746
0.00390994	-0.421847	0.000892409	-0.421847
0.00633679	-0.387949	0.00139639	-0.387949
0.00471889	-0.354051	0.00245652	-0.354051
0.00916813	-0.320153	0.00492841	-0.320153
0.0148308	-0.286254	0.010573	-0.286254
0.0297964	-0.252356	0.0220681	-0.252356
0.0680868	-0.218458	0.0465866	-0.218458
0.151948	-0.184559	0.0463903	-0.184559
0.279898	-0.150661	0.0463887	-0.150661
0.47081	-0.116763	0.0463895	-0.116763
0.689227	-0.0828644	0.000751517	-0.0828644
0.876095	-0.0489661	-1.05164e-05	-0.0489661
0.988944	-0.0150678	-6.68734e-05	-0.0150678
1	0.0188305	-1.76621e-05	0.0188305
0.891196	0.0527288	-3.7077e-05	0.0527288
0.748146	0.0866271	0.0463895	0.0866271
0.573143	0.120525	0.0463903	0.120525
0.404207	0.154424	0.0463923	0.154424
0.240933	0.188322	0.0463956	0.188322
0.13496	0.22222	0.046394	0.22222
0.0737495	0.256119	0.0465939	0.256119
0.0458406	0.290017	0.0389095	0.290017

0.0213024	0.323915	0.0180878	0.323915
0.0103816	0.357814	0.00776689	0.357814
0.00512337	0.391712	0.00356977	0.391712
0.00552784	0.42561	0.00164811	0.42561
0.00431441	0.459508	0.000921801	0.459508
0.00188756	0.493407	0.000601861	0.493407
0.00229203	0.527305	0.000459215	0.527305
0.00310098	0.561203	0.000331536	0.561203
0.00269651	0.595102	0.000288257	0.595102
0.00215721	0.629	0.000228934	0.629

Quasi-Monochromatic Data

Peak	Slit	Wings	Slit
0.00536556	-1.289	1.69439e-05	-1.289
0.00197679	-1.2551	3.38878e-05	-1.2551
0.00282398	-1.2212	-1.69439e-05	-1.2212
0.00621276	-1.18731	3.38878e-05	-1.18731
0.00338878	-1.15341	2.54158e-05	-1.15341
0.00536556	-1.11951	4.23597e-05	-1.11951
0.00197679	-1.08561	5.93036e-05	-1.08561
0.00197679	-1.05171	5.08317e-05	-1.05171
0.00621276	-1.01781	6.77755e-05	-1.01781
0.00338878	-0.983915	5.93036e-05	-0.983915
0.00451837	-0.950017	7.62475e-05	-0.950017
0.00536556	-0.916119	5.08317e-05	-0.916119
0.00197679	-0.88222	0.000110135	-0.88222
0.00536556	-0.848322	0.000110135	-0.848322
-0.000847194	-0.814424	0.000160967	-0.814424
0.000847194	-0.780525	0.000152495	-0.780525
0.00367118	-0.746627	0.000237214	-0.746627
0.00451837	-0.712729	0.000271102	-0.712729
0.00536556	-0.67883	0.000288046	-0.67883
0.00254158	-0.644932	0.000338878	-0.644932
0.00282398	-0.611034	0.000398181	-0.611034
-0.00225918	-0.577136	0.000508317	-0.577136
0.00451837	-0.543237	0.00065234	-0.543237
0.00451837	-0.509339	0.000835898	-0.509339
0.00169439	-0.475441	0.00120019	-0.475441
0.00705995	-0.441542	0.00223095	-0.441542
0.00705995	-0.407644	0.00550676	-0.407644
0.0172263	-0.373746	0.0139646	-0.373746
0.0384061	-0.339847	0.035023	-0.339847
0.0821779	-0.305949	0.0812996	-0.305949
0.170568	-0.272051	0.376055	-0.272051
0.295953	-0.238153	0.684025	-0.238153
0.448731	-0.204254	0.999994	-0.204254
0.598119	-0.170356	0.999952	-0.170356
0.768688	-0.136458	0.999935	-0.136458
0.918923	-0.102559	0.999952	-0.102559
1.00308	-0.068661	0.999986	-0.068661
1.04487	-0.0347627	1.00005	-0.0347627
1.04148	-0.0008644	1.00001	-0.0008644
1.01099	0.0330339	0.999994	0.0330339
0.960436	0.0669322	0.999994	0.0669322
0.890401	0.100831	1.00005	0.100831
0.768688	0.134729	1.00007	0.134729

0.641326	0.168627	1.00005	0.168627
0.48629	0.202525	1.00005	0.202525
0.33323	0.236424	0.854805	0.236424
0.182712	0.270322	0.48196	0.270322
0.0861314	0.30422	0.149781	0.30422
0.0401005	0.338119	0.0486177	0.338119
0.0223095	0.372017	0.0245884	0.372017
0.0155319	0.405915	0.0119991	0.405915
0.0104487	0.439814	0.00605462	0.439814
0.00169439	0.473712	0.00370789	0.473712
0.00282398	0.50761	0.00244839	0.50761
0.00169439	0.541508	0.0018836	0.541508
0.00790715	0.575407	0.00153625	0.575407
0.00197679	0.609305	0.0013188	0.609305
0.00282398	0.643203	0.00115783	0.643203
0.00367118	0.677102	0.00103923	0.677102
0.00169439	0.711	0.00088673	0.711